Sensitivity, Selectivity, and Stability of a Palladium-Loaded Single-Walled Carbon Nanotube Methane Gas Sensor

by

Melissa Keiko McGee

Submitted to the
Department of Materials Science and Engineering
in Partial Fulfillment of the Requirements for the Degree of

Bachelor of Science
at the
Massachusetts Institute of Technology
June 2017

Signature redacted

Signature of Author.....
Melissa McGee
Department of Materials Science and Engineering
April 28th, 2017

Signature redacted

Certified by.....
Michael S. Strano
Carbon P. Dubbs Professor of Chemical Engineering
Thesis Advisor

Signature redacted

Read by.....
Robert Macfarlane
Assistant Professor of Materials Science and Engineering
Thesis Reader

Signature redacted

Accepted by .....
Geoffrey Beach
Professor of Materials Science and Engineering
Chair, Department Undergraduate Committee

Sensitivity, Selectivity, and Stability of a
Palladium-Loaded Single-Walled Carbon Nanotube
Methane Gas Sensor

by

Melissa Keiko McGee

Submitted to the Department of Materials Science and Engineering
on April 28th, 2017 in Partial Fulfillment of the
Requirements for the Degree of Bachelor of Science in
Materials Science and Engineering

ABSTRACT

There exists a need to detect methane (CH_4) gas, and optical sensors provide many advantages over electronic sensors. Single-walled carbon nanotubes (SWNT) can be used as optical sensors, as SWNTs emit fluorescence upon photoexcitation. The photoluminescent (PL) intensity upon excitation depends on the electronic structure of the SWNT. Here, SWNTs are loaded with palladium (Pd) nanoparticles using sodium dodecyl sulfate (SDS). The Pd-loaded SWNTs offer a detection mechanism for methane (CH_4) by comparing the PL intensity before and after exposure to CH_4. A significant PL change (relative to the experiment) indicates a "turn-on" response to CH_4.

Preliminary experiments showed no response to CH_4 at zero and high (>10mM) Pd loading in both aqueous solution and film, indicating that there must be an optimal Pd concentration in the middle. This optimal loading for methane response was found to be in the range 2.61mM – 5.21mM Pd^{2+}.

The Pd-SWNTs in aqueous solution showed selectivity to CH_4 over nitrogen gas (N_2) and ambient air (20-22% O_2). SDS-SWNT (the control) showed a significant response to N_2 and air while Pd-SWNTs in aqueous solution showed the greatest response to methane. In film, the optimal Pd-loading (5.21mM) for sensitivity was found to exhibit an inexplicable high response to N_2 but still displayed selectivity to methane over ambient air.

Pd-SWNTs in aqueous solution and film showed stability of response over time. Pd-SWNTs in aqueous solution maintained the PL intensity with a minor decrease (3-19% decrease) in Day 14 as compared to Day 1. Pd-SWNT in aqueous solution showed turn-on response under the methane gas in Day 14. In film, the optimal Pd-loading (5.21mM) and a lower Pd-loaded SWNT (2.61mM) displayed a turn-on response to methane after 14 days, showing stability in response over time.

This work has thus demonstrated an optimally Pd-loaded SWNT that is sensitive, selective, and stable over time to methane gas.

Thesis Supervisor: Michael S. Strano
Title: Professor of Chemical Engineering

ACKNOWLEDGEMENTS

Firstly, I would like to express my deepest and sincerest gratitude to Dr. Seonyeong Kwak for her continuous support in my research efforts, and for her patience and immense knowledge. Her diligence in her research and her guidance with mine have greatly inspired and encouraged me throughout my time working with her.

I would also like to thank Professor Michael Strano for providing me the opportunity to work in the Strano Research Group as my first endeavor in scientific research. It has been a privilege working in the lab of such an accomplished and distinguished researcher.

I would also like to acknowledge Professor Robert Macfarlane as the reader of this thesis, and I am gratefully indebted to him for his very valuable comments on this thesis.

TABLE OF CONTENTS

LIST OF FIGURES

LIST OF TABLES

I. INTRODUCTION AND MOTIVATION

The need for a self-contained methane gas sensor

Detecting process gases in the atmosphere is important in relation to environmental pollution, industrial emission monitoring and process control, public security, agriculture, and a variety of other industries. Process gases are defined as any gas produced by a chemical or physical process, or a gas that is used as part of a process, often in an industrial context[1].

Methane (CH_4) gas is the main component of natural gas. Production of methane gas occurs naturally in numerous industries, including waste disposal, mining, oil and gas, and the energy sector[2]. Methane is extremely flammable, even in low concentrations and when mixed with other gases, and poses potential dangers in industry. Methane gas can be ignited by an electric spark as small as one caused by a static charge.

Methane gas leaks are the cause of numerous disasters in the coal mining industry. In January 2010, 29 men were killed in an explosion at the Upper Big Branch coalmine in Whitesville, West Virginia. Federal investigators concluded that the explosion was linked to a buildup of methane gas and coal dust in the air, and a spark ignited the explosion[3]. In June 2010, an explosion believed to have been caused by a methane gas buildup killed 16 and left dozens trapped in the San Fernando mine in Amago, Colombia[4]. Inspectors from the Institute of Geology and Mining found that the mine "didn't have gas detection devices, one of the fundamental requirements to guarantee safety in case of an explosion"[5].

In many industrial settings, it may be logistically infeasible or even dangerous to install the current source that is needed to power currently commercially available methane gas sensors. As mentioned before, an electrical spark could ignite methane gas. Thus, there is a need for a methane gas sensor that does not need a current source and can instead operate as a self-contained unit.

Carbon nanotubes as gas sensors

The basic gas sensing principle for many gas-sensing systems is the adsorption and desorption of gas molecules. Thus, a high surface area is desired in order to increase the ability for contact of the sensor and the gas molecule.

Nanoengineered materials such as carbon nanotubes (CNT) are promising because they have a greater adsorptive capacity due to their large surface area to volume ratio. Single-walled carbon nanotubes (SWNT) in particular are made of a single layer of atoms, allowing for a high level of sensitivity. Many CNT based sensors utilize the electronic properties of SWNTs. The adsorption of certain electron donating or withdrawing gas molecules onto SWNTS causes a change in conductivity that can be detected[6]. For gas molecules without electron donor or acceptor properties, SWNTs can be loaded with various metal nanoparticles that interact with the gas molecules, and a change in conductivity can be detected.

There are certain situations, however, that call for an optical rather than electronic sensing mechanism. Optical sensors have many advantages over non-optical sensors, including greater sensitivity, electrical passiveness, independence from

electromagnetic interference, wide dynamic range, and multiplexing capabilities[7]. In explosive environments, any type of electric spark may pose a hazard[8]. Thus, recent developments in SWNT based gas sensors utilize the optical properties of SWNTs. Upon photoexcitation, SWNTs emit near-infrared light. The intensity of the emission depends on the electronic structure of the SWNTs. With adsorbed gas molecules altering the electronic structure of SWNTs, a change in emission can be the detecting mechanism[9].

Proposed mechanism for methane detection

A 2002 study on transition metals demonstrated that certain metals such as rhodium (Rh), palladium (Pd), and platinum (Pt) exhibit termolecular reactions with methane[10]. However, Pd is the only transition metal that has a bound molecular precursor along the reaction pathway, and then a relatively large activation energy before the final product[11]. Thus, it is predicted that Pd forms a weakly bound intermediate complex with methane as follows:

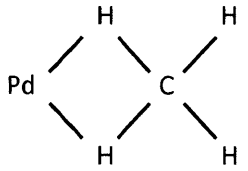

Figure 1: Intermediate palladium-methane complex
Source: Campbell, Mark L

Recent studies have demonstrated various methods for loading SWNTs. In 2010, a method of depositing and arranging Pd nanoparticles on SWNTs was demonstrated[12]. The approach first utilizes sodium dodecyl sulfate (SDS) in order to separate large bundles of SWNTs into individual tubes. Pd(II) ions are then

adsorbed onto SDS due to electrostatic interactions. Finally, UV irradiation synthesizes Pd nanoparticles by a photoreduction reaction, resulting in a helical nanostructure wrapped around the SWNTs[13].

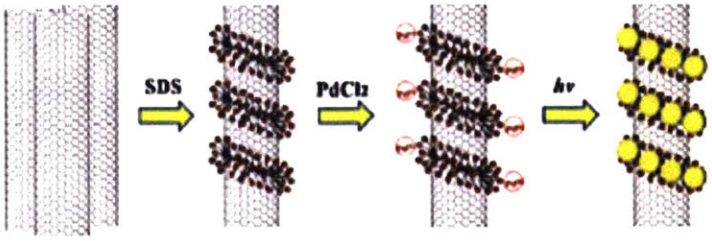

Figure 2: Approach for synthesis of ordered nanostructures of Pd nanoparticles wrapped on SWNTs
Source: Tan, Zhenquan

Thus, a methane sensor can be created using a Pd-SWNT surface. A preliminary methane sensor was configured by the NASA Ames Research Center using an electronic sensing platform. A solution of Pd loaded SWNTs was drop-deposited onto interdigitated fingers (see Figure 3), and the current through the sensor was monitored at various concentrations of methane[14].

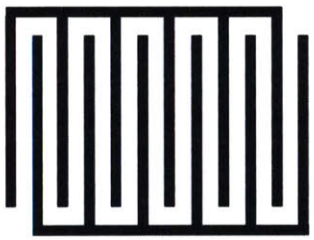

Figure 3: Schematic of interdigitated fingers
Source: McGee, Melissa

The logarithmic behavior of the conductance response to methane concentration suggests a charge transfer sensing mechanism[15]. This charge transfer mechanism is what can thus be utilized in order to optically detect methane.

In order to create an optical sensor, the same principles just described can be applied. As in previous studies, SDS can be used to functionalize SWNTs in order to uniformly deposit Pd and create Pd-loaded SWNTs[16]. The hypothesized optical methane detection process then involves several steps. First, the methane gas adsorbs at the Pd nanoparticle surface and forms the weakly bound $Pd\delta+(CH_4)\delta-$ complex (see Figure 4) as previously mentioned[17]. The methane then withdraws some electron density from the Pd nanoparticle, transferring electrons from the SWNTs to the Pd nanoparticle in order to compensate. This affects the electronic structure of the SWNT, and upon excitation, the SWNT demonstrates fluorescence.

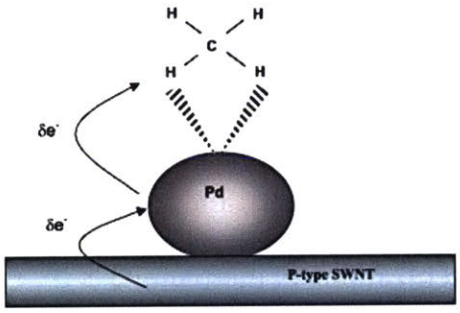

Figure 4: Proposed sensing mechanism for room temperature methane detection using Pd-SWNT sensors
Source: Lu, Yijiang

Methane gas sensor specifications for industry

The Environmental Defense Fund (EDF) has partnered with oil and gas companies, U.S. based technology developers, and other experts for the Methane Detectors Challenge (MDC) which aims to enable oil and gas companies to detect and fix methane leaks in real time[18]. Table 1 lists a selection of the specifications needed for a methane gas sensor in industry as detailed by the MDC.

Table 1: Key MDC specifications[19] for a methane gas sensor.

Specification	Industry Pilot Purchase/Deployment
Detection limits	2ppm
Detection range	2ppm – 2000 ppm
Calibration frequency	Once per year or less
Methane-specific detection	Preferred
Power consumption	As low as possible

We can see that to be useful in industry, a methane gas sensor must be very sensitive to methane, be specific to methane, and be stable over time.

Sensitivity, selectivity, and stability of the sensor

The basic criteria for a good gas sensing system include the following: (i) high sensitivity; (ii) selectivity; (iii) fast response and recovery; (iv) temperature independence; (v) stability[20].

The sensitivity of the optical methane sensor depends on numerous factors. The coverage of the Pd nanoparticles over the SWNTS is one factor that affects the sensitivity of the methane sensor. Increased Pd coverage increases the number of methane binding sites available. Our preliminary experiments have shown that the sensor response was low at both zero Pd loading and high Pd loading, implying that an optimum Pd concentration must exist in the middle. Determining this optimal Pd concentration is an important aspect of understanding the factors that affect the sensitivity of the methane sensor. In terms of sensitivity, this work will thus focus on optimizing the Pd concentration to attain a maximum response (rather than optimizing the sensor for low ppm detection) in order to lay a necessary foundation for future work.

The selectivity of the sensor to methane must also be demonstrated. Other common process gases include atmospheric air and nitrogen and it is important that the sensor has no response to these gases. Additionally, understanding the stability of the sensor is important for demonstrating the practicality of this mechanism as the eventual objective is a real-world application. Stability over time is thus necessary to explore.

The focus of this research

The three aims of this work are thus identified as follows:

Aim 1. Determine the optimal loading of palladium.

Aim 2. Demonstrate selectivity to methane.

Aim 3. Establish stability of sensor over time.

These aims will be demonstrated in both the aqueous phase and solid phase for palladium-loaded SWNTs for purposes of robustness and corroboration of the results.

II. Materials and Methods

Chemicals & Materials

Sodium dodecyl sulfate (SDS), palladium (II) chloride ($PdCl_2$) from Sigma Aldrich, HiPCO single-walled carbon nanotubes (SWNT) from Unidym, methane (CH_4) gas (>99% purity) from Airgas, nitrogen (N_2) gas (>99.9% purity) from Airgas, atmospheric air (20-22% O_2) from Airgas

Ibidi 6-channel glass microscope slide, Amicon Ultracel Regenerated Cellulose 100,000 NMWL centrifugal filters, 96-well plate

Equipment

Tip sonicator with 3mm tip (Cole Parmer), bath sonicator (Branson 2510), bench-top centrifuge (Eppendorf), UV-Visible spectrometer (Shimadzu UV-3010PC), magnetic stirring plate, 254nm UV light source, flow meter (Qubit F10)

Custom-made nIR Microscope Array

Samples loaded in a 96-well plate are placed on top of a motorized stage of a Zeiss AxioVision inverted microscope (see Appendix A.1 Methane gas sensing in aqueous phase). The samples are excited by a 785-nm photodiode laser (B&W Tek Inc.). The resulting fluorescent light is collected by a coupled nitrogen-cooled InGaAs 1D detector (Princeton Instruments) through a PI Acton SP2500 spectrometer.

Custom-made 2D nIR Fluorescence Microscope

Samples on Ibidi 6-channel glass microscope slides are placed on the stage of a Zeiss AxioVision inverted microscope (see Appendix A.2 Methane gas sensing in solid phase (film)) coupled to a nitrogen-cooled InGaAs 2D detector (Princeton Instruments) with 200mW, 785nm laser excitation (Invictus, Kaiser Optical Systemts) through ×63 objective (Zeiss, Apochromat).

Experimental Methods

Preparation of Aqueous SWNT Suspension

Raw HiPCO SWNT (Unidym, lot R0513) was processed by organic-aqueous phase separation followed by drying and homogenizing, as previously described[21].

Preparation of Pd-SWNT Solution

A 2wt% aqueous solution of sodium dodecyl sulfate (SDS) was prepared. An aqueous suspension of 2mg/mL Unidym single-walled carbon nanotubes (SWNT) was prepared. An SDS-SWNT was made by adding equal parts 2wt% SDS solution and 2mg/mL SWNT solution to create a 1mg/mL solution. The SDS-SWNT solution was placed in an ice bath and tip sonicated for 40 minutes, and centrifuged at 10,000 RPM for 60 minutes to remove aggregates. A solution of equal parts water and 1mg/mL SDS-SWNT was combined to create a 0.5mg/mL solution. SWNT concentration was calculated from absorbance measurements at 632 nm in a UV-vis-NIR scanning spectrometer using an extinction coefficient of 0.036 mg/L[22].

A 1.75mg/mL (9.87mM) solution of palladium (II) chloride ($PdCl_2$) was prepared. Various dilutions depending on the experiment (see *Solution Sets* on pages 18-19) were prepared. 200μL of each $PdCl_2$ solution was added to 1mL of the 0.5mg/mL SDS-SWNT solution and magnetically stirred for 1 hour at room temperature. The unbound palladium salts were filtrated using centrifugal filters with a membrane size of 100,000 at 1000 RPM for 2-3 minutes twice. The resulting solution was then UV irradiated at a wavelength of 254 nm for 1 hour with magnetic stirring, and centrifuged at 8,000 RPM for 30 minutes to remove aggregates. A UV absorbance measurement of each Pd-SWNT solution was performed again to determine the final SWNT concentration.

Methane gas sensing in Aqueous phase

The photoluminescent intensity was collected for each solution in aqueous phase using the custom-made nIR microscope array. 100μl of each solution was placed in a microarray well. A background spectrum of water was first taken. Each solution was then excited by a 785nm laser at an intensity of 180mV with a data collection window of 5 seconds. The photoluminescence intensity was collected for a spectrum of 945nm to 1245nm for each solution.

Methane gas was then bubbled through each solution (one at a time) for about ten minutes. The flow rate of the methane gas was controlled by a Qubit flow meter. 100μl of the solution was then immediately placed in a microarray well and photoluminescence data (with the parameters described above) was collected for each solution (see Appendix A.1 for a diagram of the experimental set up).

Methane gas sensing in Solid phase (film)

20μl of each solution was dropped onto a glass cover slide and allowed to dry overnight to create a film. The cover slide was then adhered to a 6-channel slide with an adhesive underside such that each film was placed in the middle of each channel. The custom-made 2D nIR microscope was used to continuously image the slide every 1s with an acquisition time of 1s. Methane gas was then flowed over each film in the channel for approximately 10 minutes. The flow rate of the methane gas was controlled by a Qubit flow meter (see Appendix A.2 for a diagram of the experimental set up).

Solution sets

Several separate sets of Pd-SWNTs were produced. Within a set of solutions, the varying concentrations of Pd-SWNTs were created by diluting the aqueous solution of $PdCl_2$ prior to addition to the aqueous SWNT solution. Due to centrifugation and filtering of the Pd-SWNTs, the actual concentration of palladium in the final Pd-SWNT solutions are much lower than the initially added concentration. Additionally, variability in the final concentration of palladium arises due to the inability to precisely control how much palladium is removed during the centrifugation and filtering steps. Thus, comparisons within a solution set are more valuable than comparisons between solutions sets. For this reason, solutions are often referred to by their "Sample Name" rather than their "Concentration of Pd (mM)" in this work because the numbering in the "Sample Name" gives an indication of the relative palladium concentration within the solution set.

Solution Set A (Proof of Concept)

Initial $PdCl_2$ amount (mg): 1.899mg/mL

Sample Name	Concentration of Pd^{2+} (mM)	Concentration of SWNT (mg/L)
SDS-SWNT	0.00	16.82
Pd-SWNT HI	10.7	9.53
Pd-SWNT LO	2.14	10.40

Solution Set B

Initial $PdCl_2$ amount (mg): 3.698mg/2mL

Sample Name	Concentration of Pd^{2+} (mM)	Concentration of SWNT (mg/L)
SDS-SWNT	0.00	8.12
Pd-SWNT 1	10.4	4.09
Pd-SWNT 2	5.21	5.13
Pd-SWNT 3	2.61	5.64
Pd-SWNT 4	1.30	4.82
Pd-SWNT 5	0.521	4.56

Solution Set C

Initial $PdCl_2$ amount (mg): 47.596mg/1mL

Sample Name	Concentration of Pd^{2+} (mM)	Concentration of SWNT (mg/L)
Pd-SWNT HI 1	268.4	0.54
Pd-SWNT HI 2	134.2	0.38
Pd-SWNT HI 3	67.1	0.42

Solution Set D

Initial $PdCl_2$ amount (mg): 4.450mg/2mL

Sample Name	Concentration of Pd^{2+} (mM)	Concentration of SWNT (mg/L)
SDS-SWNT	0.00	1.06
Pd-SWNT 1	3.14	0.94
Pd-SWNT 2	1.26	0.80

III. Results and Discussion

The structure of the Results & Discussion section is as follows:

- *Initial Proof of Concept* – Solution Set A
- *Optimal Palladium Concentration*
    - Aqueous solution – Solution Sets B & C
    - Solid phase film – Solution Set B
- *Selectivity*
    - Aqueous solution – Solution Set D
    - Solid phase film – Solution Set B
- *Stability*
    - Aqueous solution – Solution Set D
    - Solid phase film – Solution Set B

Initial Proof of Concept

An initial proof of concept experiment was first conducted to confirm the following:

- The addition of palladium nanoparticles quenches the photoluminescence of aqueous SWNTs.
- The addition of methane gas to the aqueous solution of Pd-loaded SWNTs allows recovery of the photoluminescence.

A set of three aqueous solutions (Solution Set A) of varying concentrations of Pd was prepared. The concentrations of Pd in each solution and the SWNT concentration is summarized as follows in Table 2:

Table 2: The concentration of Pd and SWNTs in each solution of Solution Set A.

Sample Name	Concentration of Pd^{2+} (mM)	Concentration of SWNT (mg/L)
SDS-SWNT	0.00	16.82
Pd-SWNT HI	10.7	9.53
Pd-SWNT LOW	2.14	10.40

Upon near infrared photoexcitation, the SDS-SWNT solution exhibited far greater peak intensity than the palladium-loaded SWNTS. Figure 5 shows the normalized peak photoluminescent intensity of each solution, where we can clearly see that the addition of palladium nanoparticles to SWNTs quenches the photoluminescence.

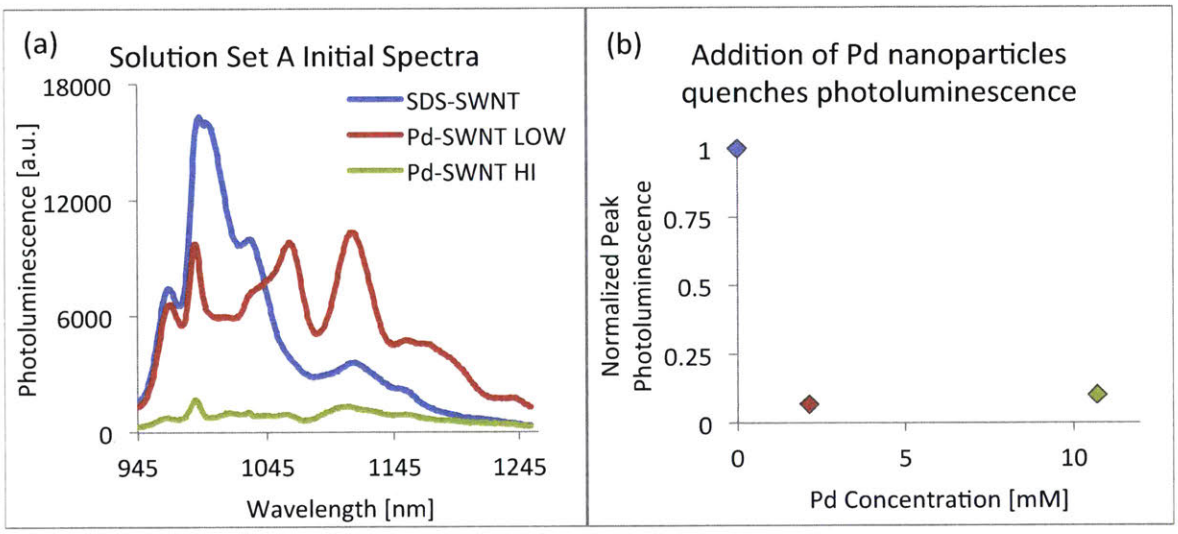

Figure 5. (a) Photoluminescence spectra and (b) Normalized peak photoluminescent intensity of the SDS-SWNT control and Pd-SWNT LOW and HI solutions.

In order to demonstrate that the addition of methane gas allows recovery of photoluminescence, methane gas was bubbled through each aqueous solution for approximately 10 minutes. These solutions were then photoexcited by a 785 nm laser. Figure 6 shows the spectra for each solution before and after bubbling methane through the solution. A photoluminescence recovery effect can clearly be seen in the low palladium-loaded SWNT solutions, providing a proof-of-concept. The SDS-SWNT control (with zero palladium loading) and the high (10.7mM) palladium-loaded SWNT solutions do not exhibit a significant response to the methane.

The percent recovery was calculated for all wavelengths and then averaged (see Appendix B.1 Calculation of Average Percent Recovery). Due to the presence of different SWNT chiralities, there are different responses at different wavelengths. Though the response at different wavelengths may give an indication of different responses for different SWNT chiralities, the scope of this work is limited to understanding whether or not there is a response to methane. The average of these percent recoveries gives a simple indication of an on/off response. We can use the SDS-SWNT response to methane as a baseline for "no response" and compare the Pd-SWNT responses to this baseline to see if there is a response to methane or not.

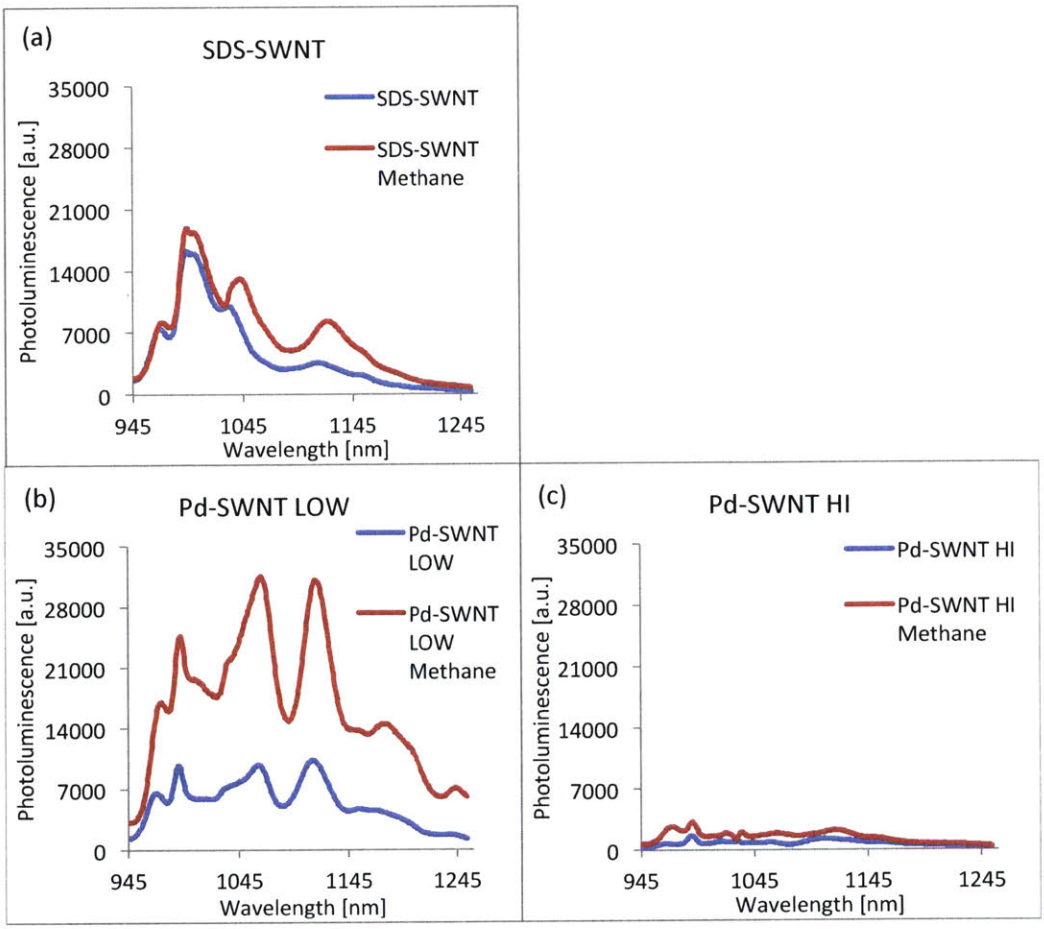

Figure 6. The photoluminescent intensity of the aqueous solution and the soluion after methane has been bubbled through (a) SDS-SWNT (the control); (b) Pd-SWNT HI with 10.7mM Pd; (c) Pd-SWNT LOW with 2.14mM Pd.

The average percent recovery[1] for the SDS-SWNT was 159% while for Pd-SWNT HI the percent recovery was 182% and for Pd-SWNT LOW it was 304%. As we can see, there is a lower response at both zero loading and at high loading of Pd than at a loading in the middle, thus indicating that there must exist an optimal concentration somewhere in the middle, near a Pd^{2+} concentration of 2.14mM.

There is a low response to methane at zero loading of Pd because the SWNTs have not been quenched, so the PL intensity before and after bubbling methane should be roughly equal. We do observe a slight recovery (159% rather than 100%); this could then establish a range of error, for photoluminescence measurements are quite sensitive. The low response to methane at a high loading of Pd may be attributable to the inability of methane to "overcome" how quenched the SWNTs are. In other words, at a high concentration of Pd, the SWNTs are fully loaded, and the fluorescence is very quenched. Thus, the methane gas may cause some "un-quenching" (an alteration of the SWNT electronic structure), but overall the response is negligible relative to how quenched the SWNT fluorescence is and thus we don't observe a high recovery. This is perhaps why we see such a distinct response at the middle loading of Pd. The SWNTs are not fully loaded, and thus the un-quenching caused by the methane gas is significant, and we observe a distinct response.

---

[1] We note that a recovery of 100% means that both spectra have the same peak intensities, indicating no response to methane.

[2] We note that the behavior of Pd-SWNT 1 is comparable to the behavior of Pd-SWNT 1 from Solution set B, even though the reported Pd concentration is lower. Similarly, the behavior of Pd-SWNT 2 is comparable to the behavior of Pd-SWNT 2/3 from Solution Set B,

Optimal Pd Concentration in Aqueous Phase

A set of five solutions (Solution Set B) of varying concentrations of Pd was prepared, with Pd-SWNT 1 having the highest concentration and Pd-SWNT 5 having the lowest concentration of palladium. The initial concentrations of Pd in each solution and the SWNT concentration is summarized below in Table 3:

Table 3: The concentration of Pd and SWNTs in each solution of Solution Set B.

Sample Name	Concentration of Pd^{2+} (mM)	Concentration of SWNT (mg/L)
SDS-SWNT	0.00	8.12
Pd-SWNT 1	10.4	4.09
Pd-SWNT 2	5.21	5.13
Pd-SWNT 3	2.61	5.64
Pd-SWNT 4	1.30	4.82
Pd-SWNT 5	0.521	4.56

We can again see the quenching effect of the palladium in the initial spectrum of the Pd-SWNTs in Figure 7. At a high level of Pd loading, the PL intensity is low, and at zero Pd loading, the PL intensity is high.

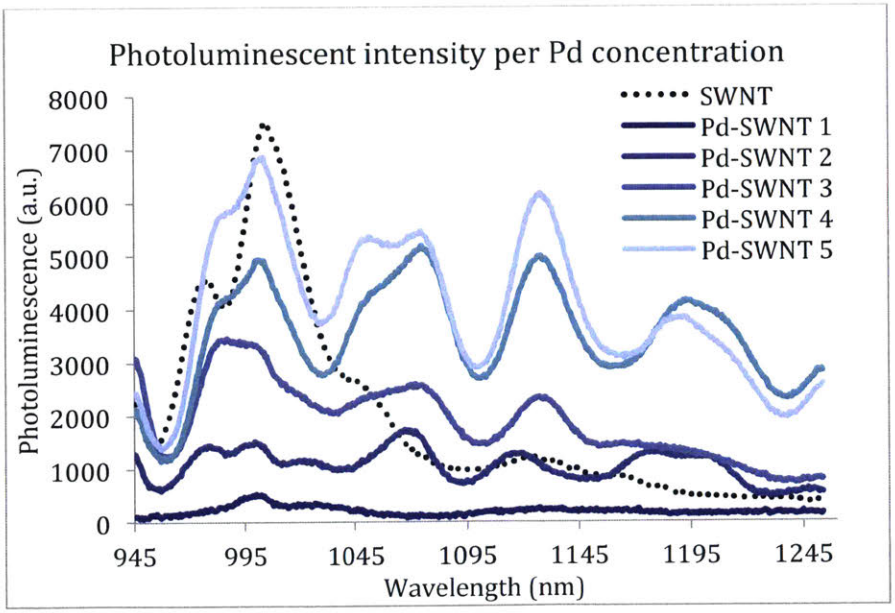

Figure 7. Photoluminescent intensity of each Pd concentration.

In order to more clearly see this effect, we can normalize the peak PL intensity of each solution to the control (SDS-SWNT). As shown in Figure 8, the PL intensity decreases with an increasing Pd concentration.

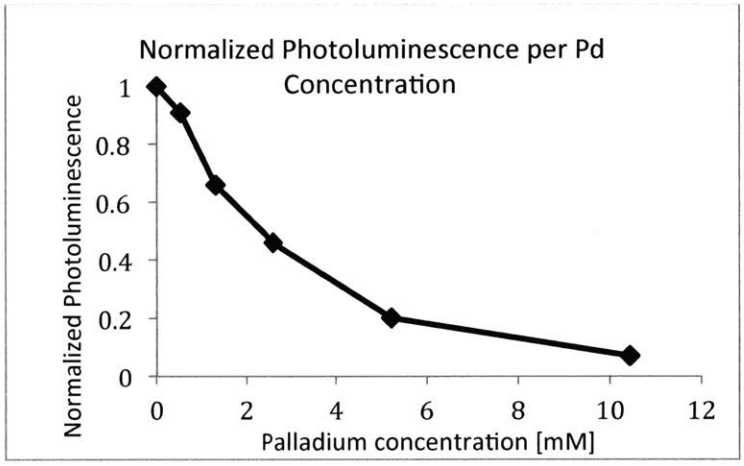

Figure 8: Normalized photoluminescent intensity for each Pd concentration.

The PL intensity was again collected after bubbling methane gas through each solution for 10 minutes (see Appendix C.1, Solution Set B Aqueous Phase response to methane gas). The average percent photoluminescence recovery for each solution was calculated. The results in Figure 9 (additionally including the results from Solution Set A from the initial proof of concept) clearly show an optimal recovery for aqueous solutions at a Pd^{2+} concentration of 5.21mM.

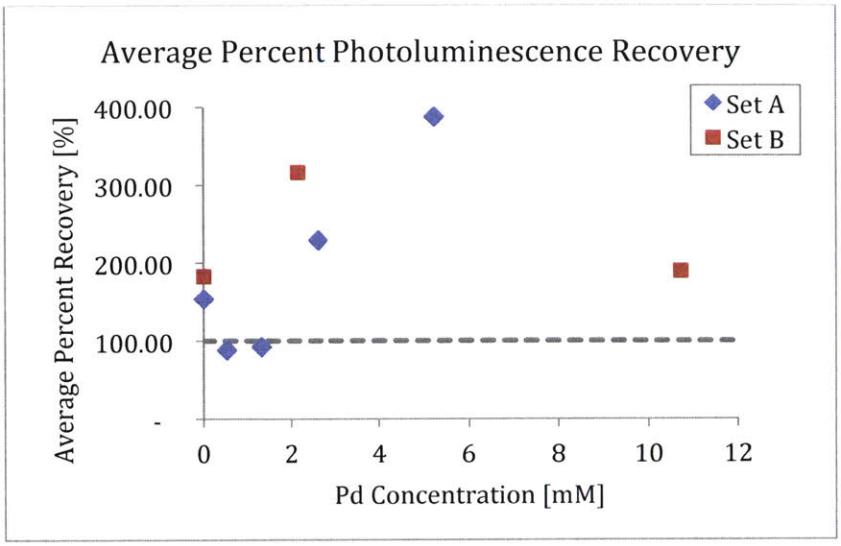

Figure 9: Average percent photoluminescence recovery for each palladium concentration. The dashed line at 100% indicates no response to methane.

An additional experiment was conducted to indeed confirm that an extreme higher loading of palladium nanoparticles does not lead to better detection of methane gas. A set of palladium-loaded SWNTs (Solution Set C) was prepared with very high palladium concentrations.

Table 4: The concentration of Pd and SWNTs in each solution of Solution Set C.

Sample Name	Concentration of Pd^{2+} (mM)	Concentration of SWNT (mg/L)
Pd-SWNT HI 1	268.4	0.54
Pd-SWNT HI 2	134.2	0.38
Pd-SWNT HI 3	67.1	0.42

Figure 10 shows that these solutions observed no initial photoluminescence upon near infrared photoexcitation, and additionally no photoluminescence recovery after bubbling methane through the solution. The absence of initial photoluminescence and also photoluminescence recovery may be attributable to the fact that the SWNT concentration for these solutions was extremely low. The average SWNT concentration for Solution Sets A and B was 7.68 (±4.12) mg/L. The

average SWNT concentration for Solution Set C was much lower at 0.45 (±0.085) mg/L. A possible explanation for the extremely weak photoluminescence of these Set C solutions is that the highly palladium-loaded SWNTs were sediment during purification because palladium is a dense metal.

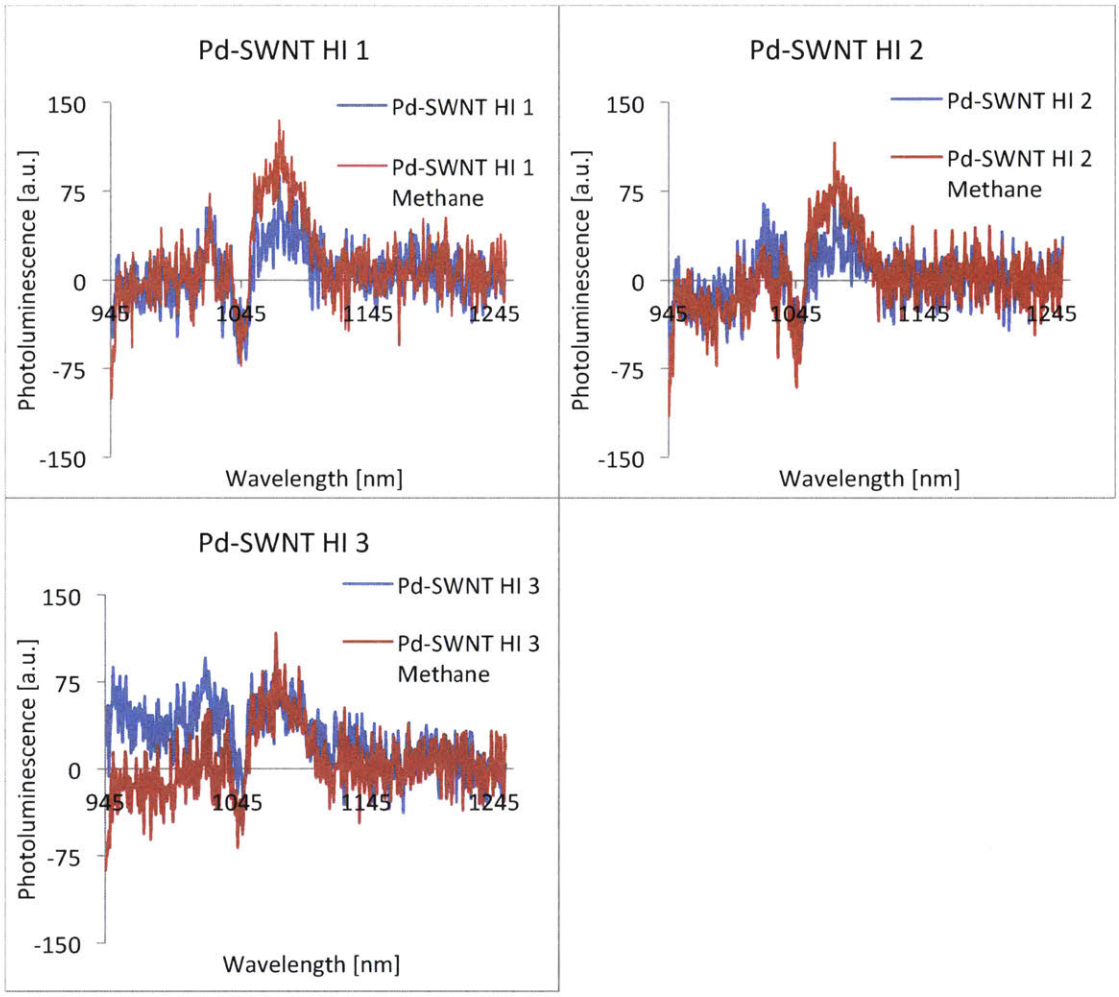

Figure 10: Pd-SWNT solutions at a high concentration of Pd see no initial photoluminescence and additionally no response to methane.

It is thus proven both zero and high loading of palladium have low sensitivity to methane gas in aqueous solution, with an optimal Pd^{2+} concentration existing in the middle at an initial concentration of 5.21 mM.

Optimal Pd Concentration in Film

Solution Set B was then tested in film form (see Materials & Methods, *Solid phase (film)* for description of protocol). The fluorescent emission was collected using the custom-made 2D nIR fluorescence microscope with continuous laser excitation of the sample using a 1s collection window every 1s. After focusing for maximum fluorescence, methane gas was flowed through the microchannel over each film for approximately 10 minutes, with photoluminescence being continuously collected at 2 s/frame. The average photoluminescence per frame was calculated using ImageJ in order to determine the photoluminescence over time.

Direct quantitative comparison of the resulting data is more difficult in film, for the absolute value of the resulting data is arbitrary due to the inconsistency while focusing the microscope used to collect data. Thus, the important quantity for comparison is the height of the response to methane, for regardless of the initial absolute value of the photoluminescence, the difference in photoluminescence due to the addition of methane can be directly compared. The PL intensity data for Pd-SWNTs in film are normalized by the same scale within a figure (separate figures have different normalization scales) in order to allow for direct comparison of the difference in photoluminescence over time (see Appendix B.2, Calculation of fluorescence of solid phase (films)) within a figure.

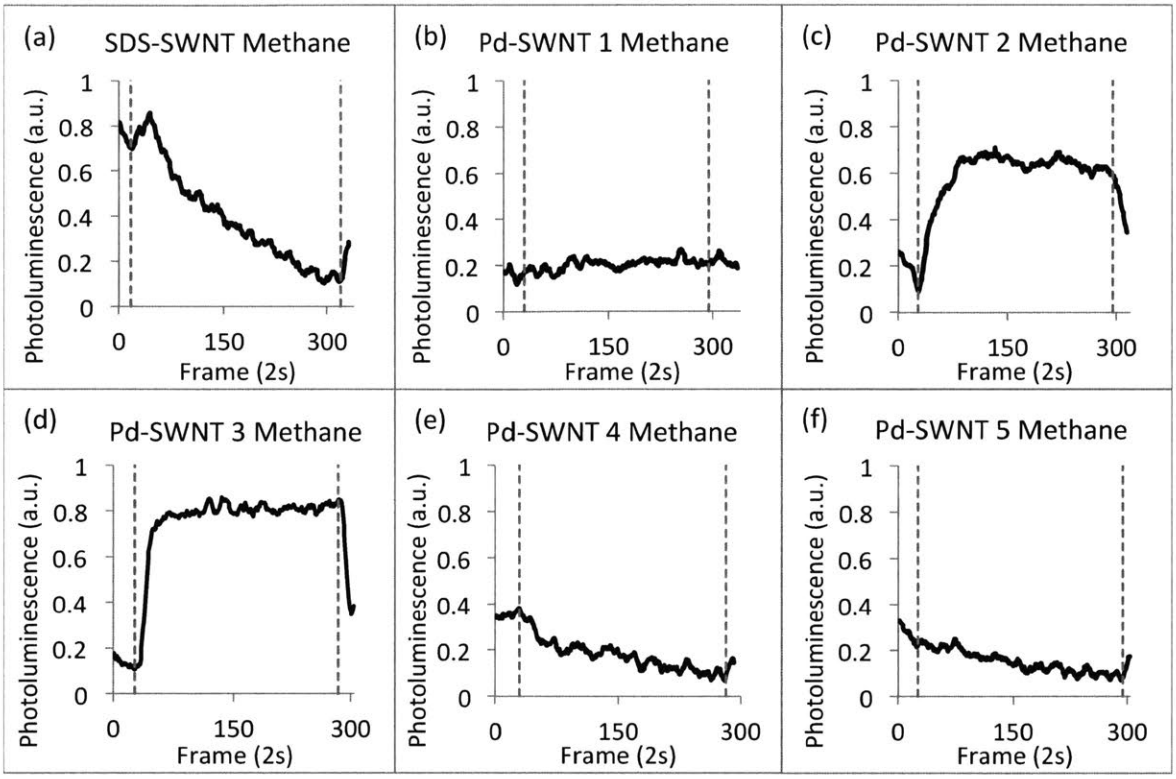

Figure 11: Photoluminescent intensity of Pd-SWNT film over time for (a) SDS-SWNT; (b) Pd-SWNT 1; (c) Pd-SWNT 2; (d) Pd-SWNT 3; (e) Pd-SWNT 4; (f) Pd-SWNT 5. Dashed lines indicate when methane gas flow starts and stops. Normalized by a factor of 400 a.u.

We can see that Pd-SWNT 2 (5.21 mM Pd^{2+}) and Pd-SWNT 3 (2.61mM Pd^{2+}) have a clear response to methane gas; in particular, Pd-SWNT 3 has the greatest and most distinct response. We also see that the SDS-SWNT sample has a distinct downward sloping trend over time, and Pd-SWNT 4 and 5 (which have a very low Pd loading, 1.30mM and 0.521mM respectively) also demonstrate this downward trend. This may be because the flow of methane may agitate the film of SWNTs, causing it to become consistently out of focus over time, leading to lower fluorescence. This effect could be mitigated in future work by reducing the flow of gas; this work focuses simply on an on/off response, but future work on this material that aims to

reduce the detection limit to as low as 2ppm would use a much lower flow rate of gas so this effect would most likely not be observed.

In film, the response to methane gas follows a similar trend as the aqueous solution, with no response at zero and high loading (>10.4mM) of palladium, and a distinct response at Pd concentrations in the middle. The reason for this maximum response at a middle loading is most likely due to the same reason as previously discussed. At zero/low loading, the SWNTs are not notably quenched by Pd, and thus there isn't much of a response to methane. At a high loading, the un-quenching is relatively small to how quenched the SWNTs are due to the high loading of Pd. At a middle loading, the un-quenching due to the methane gas is significant relative to how loaded the SWNTs are. Pd-SWNT 3 (2.61mM Pd^{2+}) showed better sensitivity compared to Pd-SWNT 2 (5.21mM Pd^{2+}) as the aqueous testing proposed.

The difference in results may be due to the difference in dispersion of SWNTs in aqueous solution versus in film. The SDS-SWNT and Pd-SWNT films were formed by the evaporation of drops on a nonporous glass substrate. As the drop dries, the evaporation of the solvent leads to an increase in the concentration of the suspended SWNT solution at the free surface[23]. This forms a "crust"[24] at the free surface which then becomes the thin film once all of the solvent has evaporated. This crusting leads to a higher concentration of SWNTs in film than in aqueous solution and it thus makes sense that the trend for the films is shifted to lower concentrations compared to the aqueous solutions. The trend observed in aqueous solution thus remains consistent.

Selectivity of Pd-SWNTs in Aqueous Solution

A set of two Pd-SWNT aqueous solutions (from Solution Set D) and an SDS-SWNT control were tested for selectivity by bubbling methane, nitrogen, and ambient air through the solutions for ten minutes each. Only the solutions with Pd concentrations that exhibited a response to methane were tested for selectivity. As noted in Materials and Methods, *Solution Sets*, the final Pd loading has great variability due to the processing method. Thus, a range of Pd solutions was made and the two Pd-SWNT solutions with behavior similar to the original optimal concentration were selected.

Table 5 below shows the Pd^{2+} and SWNT concentrations of the solutions used for selectivity testing[2].

Table 5: The concentration of Pd and SWNTs in each solution of Solution Set D.

Sample Name	Concentration of Pd^{2+} (mM)	Concentration of SWNT (mg/L)
SDS-SWNT[3]	0.00	1.06
Pd-SWNT 1	3.14	0.94
Pd-SWNT 2	1.26	0.80

Figure 12 shows that the SDS-SWNT control has a high response to both nitrogen and air, while it has a minimal response (84.6% photoluminescence recovery) to methane (as seen in previous experiments). The Pd-loaded SWNTs also have a

[2] We note that the behavior of Pd-SWNT 1 is comparable to the behavior of Pd-SWNT 1 from Solution set B, even though the reported Pd concentration is lower. Similarly, the behavior of Pd-SWNT 2 is comparable to the behavior of Pd-SWNT 2/3 from Solution Set B, even though the reported Pd concentration is lower.

[3] The response to methane was tested on a different day than the responses to nitrogen and air, so both SDS-SWNT spectra (a and b in Figure 12) are shown for respective comparison

reaction to nitrogen and air, but the reaction is much smaller in magnitude as compared to the response to methane.

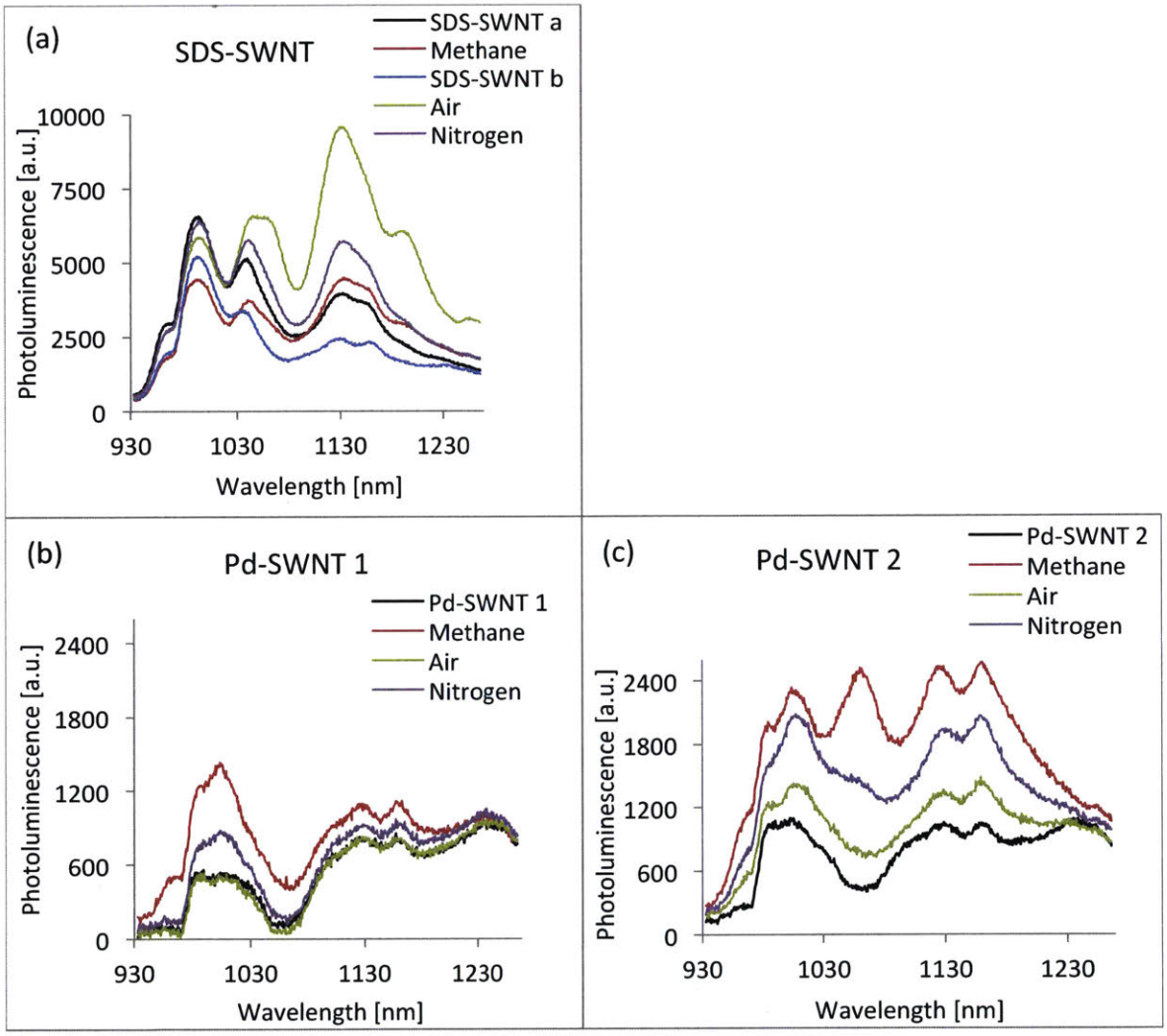

Figure 12: Change of PL intensity under the presence of various gases (a) SDS-SWNT; (b) Pd-SWNT 1; (c) Pd-SWNT 2

Pd-SWNT 2, with a lower Pd loading than Pd-SWNT 1, demonstrates a greater response to nitrogen and air than Pd-SWNT 1 (see Table 6 for average percent recovery). This makes sense, for SDS-SWNT, without Pd loading, demonstrates a distinct PL change to air and nitrogen. The electronic properties of SWNTs are highly sensitive to oxygen exposure[25]. As previously mentioned, the

photoluminescent intensity of emission depends on the electronic structure of SWNTs and thus the SDS-SWNT solution exhibits a response to air (composed of ~20% oxygen). Palladium, however, does not react with oxygen under normal ambient conditions and thus it makes sense that the more highly Pd-loaded solution has no response to air.

Table 6. Average percent recovery to methane, air, and nitrogen.

	Average Percent Recovery		
Sample	Methane	Air	Nitrogen
SDS-SWNT	84.6%	231.6%	175.0%
Pd-SWNT 1	173.3%	97.8%	127.6%
Pd-SWNT 2	315.3%	144.2%	233.0%

The response to nitrogen is harder to understand. One possible explanation is that the nitrogen source may contain nitrous oxide (NOx) contaminants. Previous work with SWNTs has shown that the electronic structure of SWNTs are modified by the charge transfer between the SWNT surface and nitrous oxides, resulting in a response to nitrous oxides[26].

Another possible explanation is that the act of agitating the solution itself produced a response. The initial photoluminescence of the solutions were collected on a later date than the creation of the solutions; it is possible that some settling occurred, and thus the initial photoluminescence is much lower than if the solution were agitated immediately prior to data collection. The bubbling of the air and nitrogen agitated the solution, dispersing the SWNTs throughout the volume of the solution and possibly contributing to a greater photoluminescence upon photoexcitation.

These results also show that different molecules have different effects on the electronic properties of the SWNTs. Specifically, we see a different PL response for different gases at different wavelengths, which corresponds to different SWNT chiralities. Though outside the scope of this work, it may be that certain chiralities are more selective to methane over air/nitrogen, while other chiralities may be less selective. Future experiments could focus on establishing which chiralities respond the most to methane, air, and nitrogen by testing solutions composed only of each of the different SWNT chiralities with each of the gases.

Though the 1.26mM Pd-loaded SWNT solution had a response to nitrogen and air, the response to methane is still the most distinct and greatest in magnitude. Thus, the Pd-SWNT solution is still selective to methane, especially if higher concentrations (3.14mM) of palladium are used.

Selectivity of Pd-SWNTs in Film

Solution Set B was tested in film form under a constant flow of nitrogen and air. The fluorescent emission was collected using an nIR microscope array with continuous laser excitation of the sample using a 1s collection window every 1s. After focusing for maximum fluorescence, nitrogen and then air was each flowed through the channel over each film for approximately 10 minutes, with photoluminescence frames being continuously collected every 2 seconds. The channels were purged with air for 2 minutes and then no gas was flowed for 2 minutes between trials. The average PL intensity per frame was calculated using ImageJ in order to determine the photoluminescence over time.

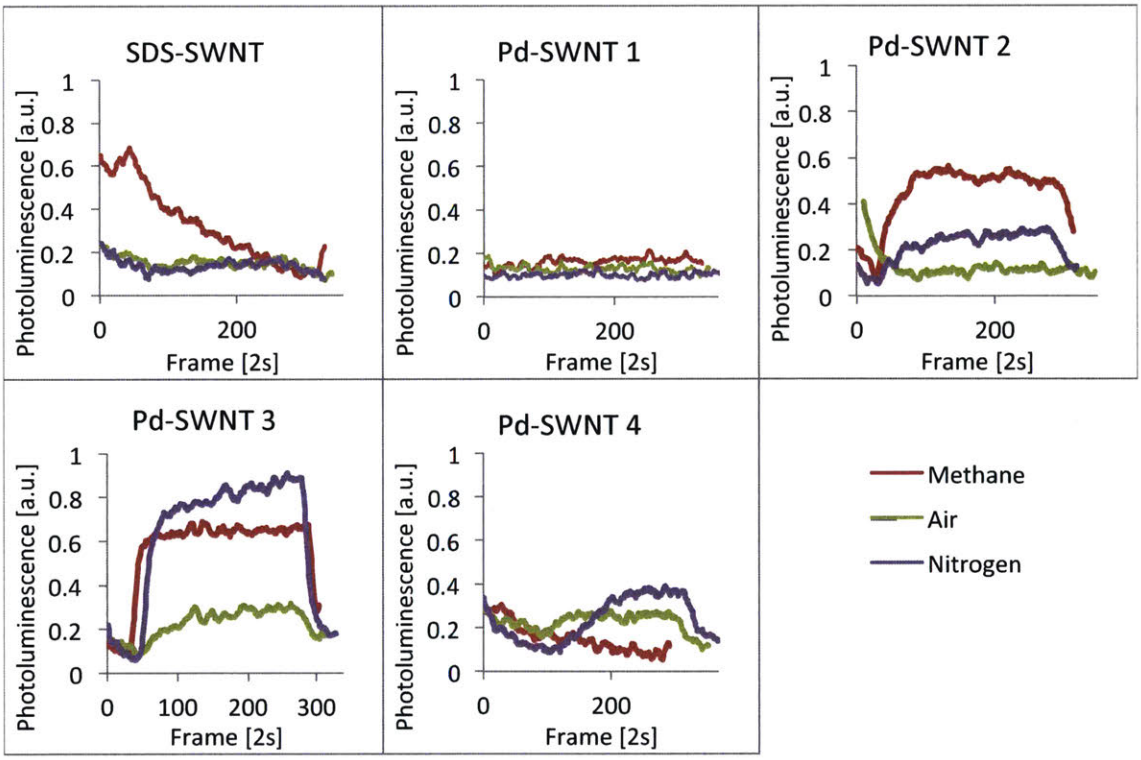

Figure 13: Normalized photoluminescence over time of films (a) SDS-SWNT; (b) Pd-SWNT 1; (c) Pd-SWNT 2; (d) Pd-SWNT 3; (e) Pd-SWNT 4. Films continuously imaged using custom-made 2D nIR microscope at a rate of 1 frame/2s. Each gas was flowed over each film in the channel for approximately 10 minutes. The flow rate of the methane gas was controlled by a Qubit flow meter. Normalized by a factor of 500 a.u.

Pd-SWNT 2 (5.21mM Pd^{2+}) and Pd-SWNT 3 (2.61mM Pd^{2+}) demonstrated a significant change in PL intensity in the presence of nitrogen; Pd-SWNT 2 did not demonstrate a response to air while Pd-SWNT 3 did (see Figure 13). In both cases, the response was greater and more distinct with Pd-SWNT 3 than with Pd-SWNT 2. This may be due to the fact that Pd-SWNT 3 is less loaded with Pd and thus the greater response may be due to the availability of non-Pd-loaded SWNTs for reacting with the gases.

Figure 13 above seems to indicate that the SDS-SWNT film does not have a response to nitrogen and air. However, as explained, the direct comparison is shown simply to compare the magnitude of responses to the gases. We can focus on the behavior of the SDS-SWNT film alone (on its own normalized scale) in order to understand better.

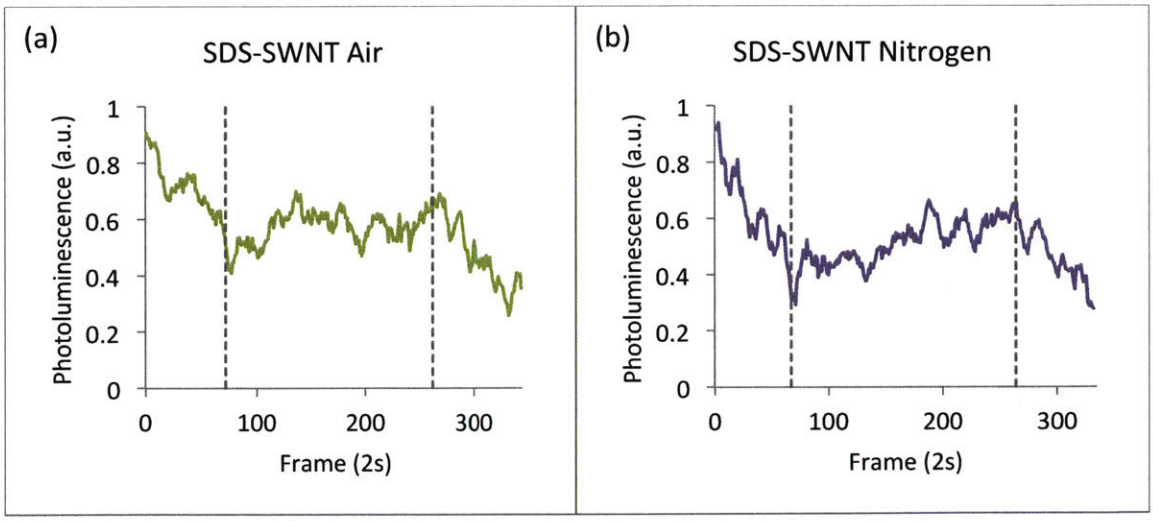

Figure 14. Normalized photoluminescence of the SDS-SWNT film under (a) air and (b) nitrogen gas flow. Normalized by a factor of 130 a.u.

As we saw with the methane gas previously, there is a consistent decreasing trend in the photoluminescence for the SDS-SWNT film. However, the addition of the air and nitrogen disrupt this trend, showing that the SDS-SWNT film reacts enough to these gases (i.e. the photoluminescence increases) such that the otherwise decreasing trend is instead flat, indicating a response to nitrogen and air. Thus, as in the aqueous solution, we see that SDS-SWNT responds to nitrogen and air, though in not as great of a magnitude as Pd-SWNT 2 and 3.

If we focus in on the behavior of the 10.4mM palladium-loaded film, Pd-SWNT 1, we observe no response to nitrogen and air. Thus, the data for the solid (film) phase remains consistent with the results from the aqueous phase with respect to the presence of a response to nitrogen and air for SDS-SWNT and the absence of a response to nitrogen and air for a highly Pd-loaded SWNT.

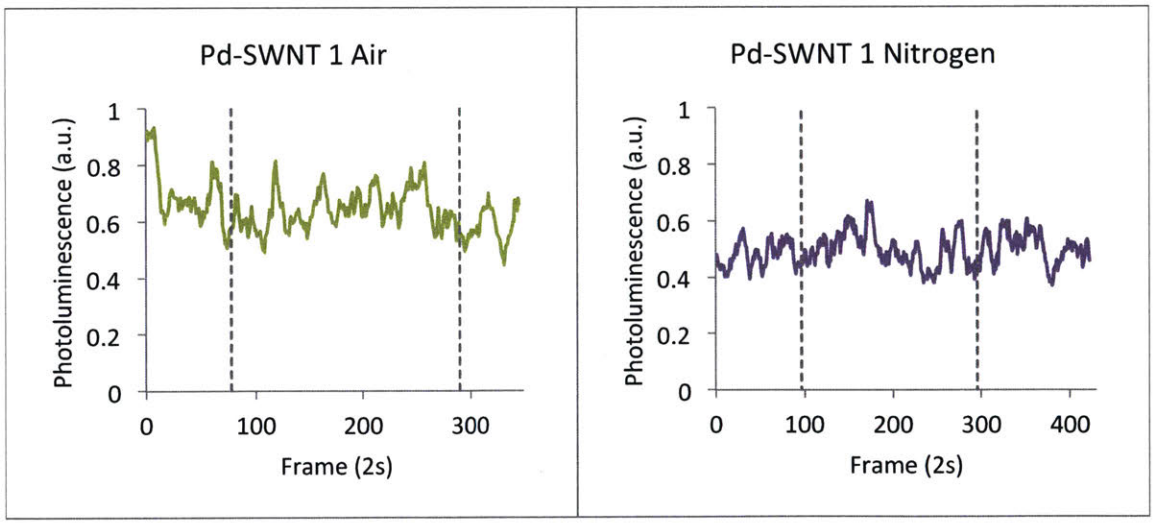

Figure 15: Normalized photoluminescence of the Pd-SWNT 1 film under (a) air and (b) nitrogen gas flow. Normalized by a factor of 100 a.u.

The data show the response to nitrogen and air follows the trend similar to the response to methane gas, where none and high loading (10.4mM) of palladium have a lower response than a middle loading (2.61mM to 5.21mM). The response of the films to air can be explained by the previously explained SWNT response to oxygen. However, the response to nitrogen cannot be attributed to agitation as in the aqueous solutions. There may exist some unknown other mechanism that causes a response to nitrogen. Future experiments that focus on wavelength-specific responses may aid in the exploration of this mechanism.

We can see that the higher the palladium loading, the less the response to nitrogen and air. However, as previously determined, a higher palladium loading is less sensitive to methane than a middle loading. Thus, there exists a tradeoff between sensitivity and selectivity.

Stability of Pd-SWNTs in Aqueous Solution

A set of two Pd-SWNT aqueous solutions (from Solution Set D) and an SDS-SWNT control were tested for stability. An initial response to methane (recorded as Day 1 in Figure 16 below) was first tested, and the response to methane was tested again on Day 14. The Pd-SWNT solutions were stored at room temperature.

Figure 16 below shows that for the SDS-SWNT control, there is no response to methane (<10% difference). However, the PL intensity of the SDS-SWNT solution decreases over time. For Pd-SWNT 1 and Pd-SWNT 2, we see that the spectra of the initial solution and the solution after two weeks are roughly the same.

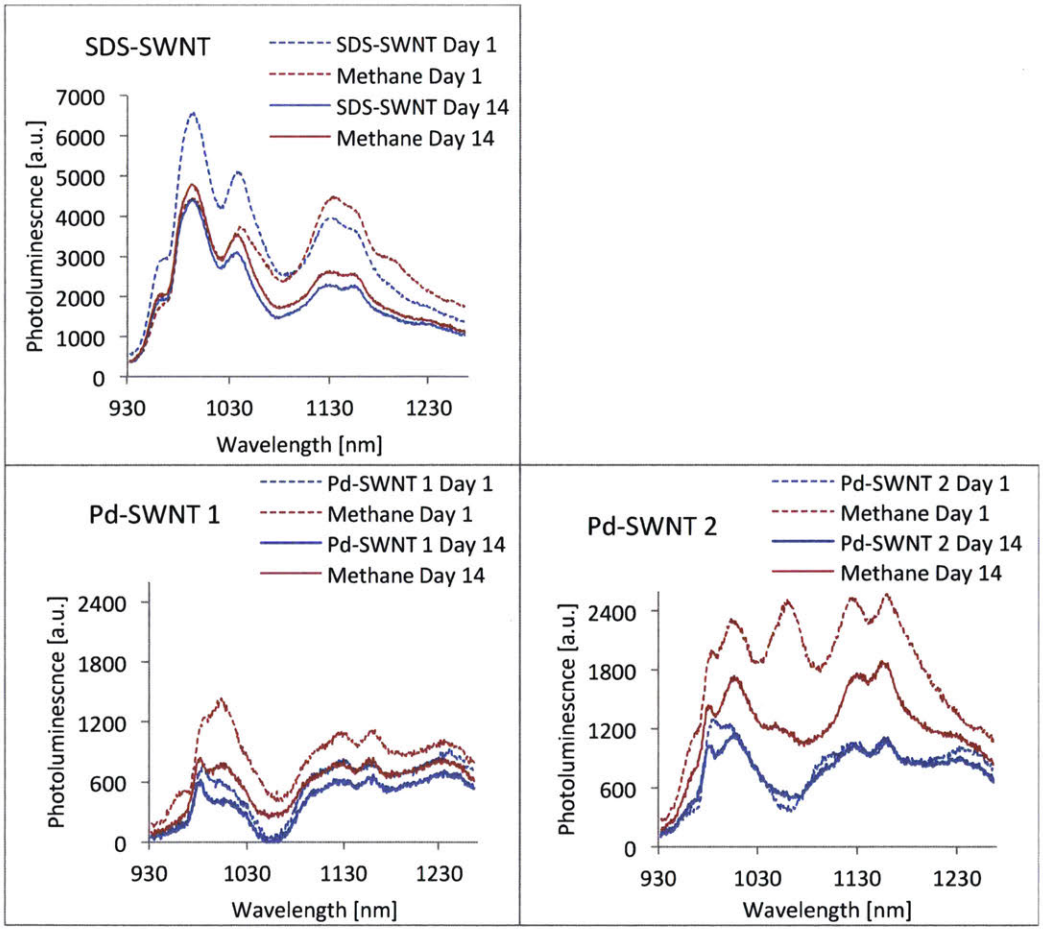

Figure 16: Response to methane on Day 1 and Day 14 of (a) SDS-SWNT; (b) Pd-SWNT 1; and (c) Pd-SWNT 2

The PL intensity of SDS-SWNT dropped by 40% in Day 14 as compared to that of Day 1; however, Pd-SWNTs maintained the PL intensity with minor decrease (3-19%) in Day 14 (see Table 7). Both the Pd-SWNT 1 (with 3.14mM Pd^{2+}) and Pd-SWNT 2 (with 1.26mM Pd^{2+}) aqueous solutions showed turn-on response under methane gas in Day 14.

Table 7: Comparison in PL intensity and response to methane of SDS-SWNT, Pd-SWNT 1, and Pd-SWNT 2 aqueous solution between Day 1 and Day 14.

Sample	% of PL in Day 14[a]	Response[b] to CH_4 in Day 1	Response[b] to CH_4 in Day 14	Change in % response
SDS-SWNT	62%	-	-	-
Pd-SWNT 1	81%	152%	128%	-24%
Pd-SWNT 2	97%	243%	164%	-79%

[a] Compared to Day 1

[b] Turn-on response

We note an interesting effect, where the addition of Pd seems to stabilize the aqueous solution of SWNTs. The highly palladium-loaded Pd-SWNT 2 solution maintains 97% of the initial photoluminescence after 14 days compared to just 62% for the zero Pd-loaded SDS-SWNT solution. This may be due to the nature of the SDS-SWNT interaction. SDS has a 12-carbon hydrophobic tail attached to a sulfate group. The hydrophobic tail is attracted to the SWNT, forming an ordered supramolecular self-assembly on the SWNT surface[27]. The SWNTs are thus dispersed in aqueous solution by the electrostatic repulsion from the polar heads.

Figure 17: Ordered supramolecular assembly of SDS on a SWNT
Source: Tan, Zhenquan

This ordered assembly and hence SWNT dispersion is held together only by hydrophobic interactions. With the addition of Pd nanoparticles, it is possible that the SDS assembly on the SWNTs is "held" in place due to the very strong, ionic attraction between the anionic SDS head and the positively charged Pd ion.

Figure 18: Ordered supramolecular assembly of Pd nanoparticles on SDS on a SWNT
Source: Tan, Zhenquan

Thus, the addition of Pd may stabilize the SDS assembly which then keeps the SWNTs uniformly dispersed in aqueous solution. Individual SWNTs would otherwise interact with each other strongly due to van der Waals forces and aggregate into bundles[28].

Another trend we observe from the results is that although Pd-SWNT 2 has a higher sensitivity to methane at both Day 1 and Day 14 than Pd-SWNT 1, the relative decrease in sensitivity to methane is higher for Pd-SWNT 2. It may be that over time, some Pd nanoparticles may become detached from the SWNTs; the SWNTs would still remain properly dispersed, so the initial spectra would remain unchanged, but upon bubbling the solution with methane, the detached Pd nanoparticles would have a greater surface area for interaction with the methane, and thus the methane would have less of an effect on the Pd-loaded SWNTs. This would affect Pd-SWNT 2 more than Pd-SWNT 1 because Pd-SWNT 2 has a lower Pd loading. There is thus another tradeoff, where a higher concentration of Pd stabilizes the Pd-SWNT solution, but also has a greater relative decrease in sensitivity to methane over time.

Stability of Pd-SWNTs in Film

Pd-SWNT 2 (with 5.21mM Pd^{2+}) and Pd-SWNT 3 (with 2.61mM Pd^{2+}) from Solution Set B were tested in film form under a constant flow of methane on Day 1 and again on Day 14. The Pd-SWNT films were stored at room temperature. During each test, the fluorescent emission was collected using an nIR microscope array with continuous laser excitation of the sample using a 1s collection window every 1s. After focusing for maximum fluorescence, methane gas was flowed through the channel over each film for approximately 10 minutes, with photoluminescence frames being continuously collected every 2 seconds. The average PL intensity per frame was calculated using ImageJ in order to determine the photoluminescence over time.

We normalize the results on the same scale in order to be able to compare the magnitude of the response to methane. Because SDS-SWNT does not have a response to methane, we did not look at the stability of the SDS-SWNT film over time, but we can compare the Pd-SWNT 2 and Pd-SWNT 3 films.

We see in Figure 19 that Pd-SWNT 2 showed a delayed response to methane, while Pd-SWNT 3 still displayed an immediate turn-on response even after 14 days.

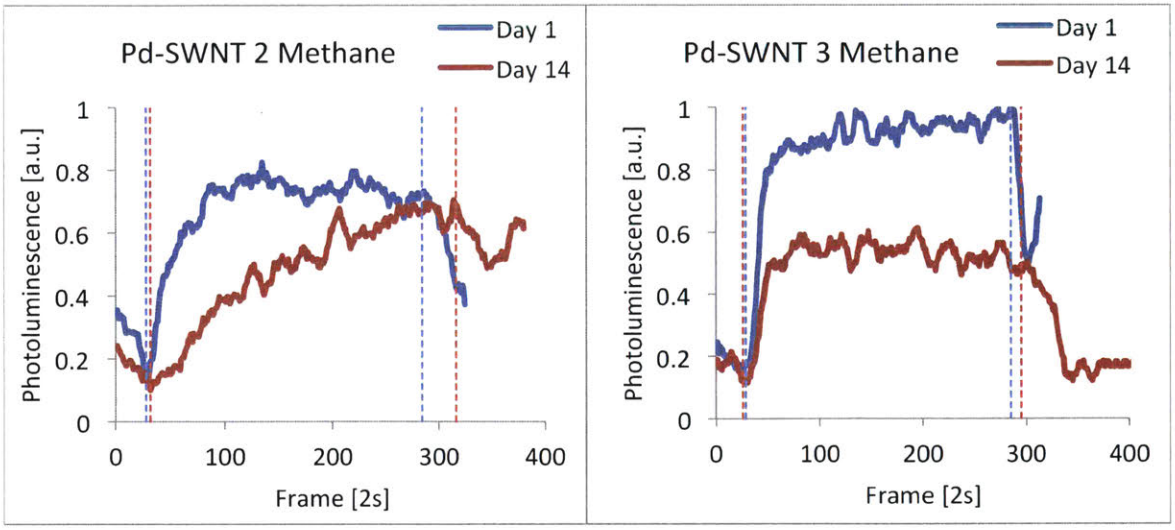

Figure 19: Normalized photoluminescence over time of (a) Pd-SWNT 2 and (b) Pd-SWNT 3; dashed lines indicate when methane flow starts and stops. Normalized by a factor of 264 a.u.

This is most likely due to the fact that the response after 14 days is a function of the initial response. Pd-SWNT 2 originally had a weaker, less distinct response while Pd-SWNT 3 had a more distinct initial response due to reasons previously discussed (see Optimal Pd Concentration in Film). Thus, after 14 days, the responses follow the initial trend.

Summary

In this work, it was shown that the addition of palladium nanoparticles quenches the photoluminescence of aqueous SWNTs, and the addition of methane gas to the aqueous solution of Pd-loaded SWNTs allows recovery of the photoluminescence in both aqueous solution and solid phase (film).

Preliminary experiments showed no response to methane at zero and high (>10mM) Pd loading in both aqueous solution and in film, indicating that there must be an optimal Pd concentration in the middle. This optimal loading for methane response was found to be in the range 2.61mM – 5.21mM Pd^{2+}.

The Pd-SWNTs in aqueous solution also showed selectivity to methane. SDS-SWNT showed a significant response to nitrogen and air and thus lower-loaded (1.26mM) Pd-SWNTs showed a response to nitrogen and air, while higher-loaded (3.14mM) Pd-SWNTs showed a lower response to nitrogen and air. Both Pd-SWNT solutions showed the greatest response to methane despite having responses to nitrogen and air. In film, the optimal Pd-loading (5.21mM) was found to exhibit an inexplicable high response to nitrogen but still displayed selectivity to methane over ambient air.

Pd-SWNTs in aqueous solution and film showed stability of response over time. In aqueous solution, the PL intensity of SDS-SWNT dropped by 40% in Day 14 as compared to that of Day 1; however, Pd-SWNTs maintained the PL intensity with minor decrease (3-19%) in Day 14. Both Pd-SWNT 1 and Pd-SWNT 2 in aqueous solution showed turn-on response under the methane gas in Day 14. In film, the

optimal Pd-loading (5.21mM) displayed a turn-on response to methane after 14 days, showing stability in response over time.

This work has thus demonstrated an optimally Pd-loaded SWNT that is sensitive, selective, and stable over time to methane gas.

IV. Conclusion

This work has shown that Pd-loaded SWNTs can be used as a sensitive, selective, and stable sensor for methane gas, thus establishing a valuable foundation for further work in this field in order to fully develop a methane gas sensor that is usable in industry. As previously mentioned, there exists a need to detect methane gas subject to a certain set of conditions that current detection systems do not satisfy, either in part or in full. This Pd-SWNT system meets, at a basic level, all of the desired characteristics – sensitive, selective, and stable optical detection – with the potential for being further developed to meet all required industry criteria. These criteria include, but are not limited to: detection range of 2 – 2,000ppm, annual calibration frequency, remote calibration, ability to measure other hydrocarbons, methane-specific detection, low power consumption, temperature range of -20F to 135F, and an expected lifetime of 10 years[29].

Testing in the aqueous phase showed that there are different responses at different wavelengths due to the different SWNT chiralities. Though fully investigating this effect was outside the scope of this work, future work could focus on utilizing these responses to further tailor the sensor. There may be different responses to different molecules at different SWNT chiralities. This is especially important in the oil and gas industry, for current sensors are often limited by their inability to selectively determine a singular compound within a mixture of gases[30]. If a Pd-loaded sensor could selectively respond to different hydrocarbons at different SWNT chiralities, then a single sensor could accurately detect many different compounds.

This work focused on the sensor response at a constant concentration/flow of methane gas. However, it is important in industry to have a detection range for methane gas of 2 – 2,000ppm. Future work should thus focus on establishing the sensitivity, selectivity, and stability of the response of the sensor at different concentrations and flow rates of methane gas.

Additionally, the concentration of SWNTs in different samples was recorded but not controlled. A lower SWNT concentration may reduce the noise in the response, especially in film. A film consisting of a single layer of homogeneously dispersed Pd-SWNTs would ensure that the response is not affected by other SWNTs. This could allow for a highly sensitive sensor, even down to the single-molecule level.

This work investigated the stability of the sensor over time, but stability over a range of other factors is also needed for industry. Future work should thus focus on stability over a range of environmental conditions (such as temperature, humidity, and pressure).

The detection of methane gas is vital across industries, especially for environmental reasons in the oil & gas industry and for safety reasons in the mining industry. This work has shown that there is compelling potential to fulfill the various requirements needed for a methane gas sensor and with due effort and persistence, there is great confidence that future work can build upon this research to comprehensively achieve these needs.

V. REFERENCES

[1] Cleaver, Kevin David. "The analysis of process gases: a review." *Accreditation and Quality Assurance: Journal for Quality, Comparability and Reliability in Chemical Measurement* 6.1 (2001): 8-15.
[2] "Detecting the Dangers of Methane Gas Leaks." *Heating and Process.* N.p., 22 Nov. 2016. Web. 07 Feb.
[2] "Detecting the Dangers of Methane Gas Leaks." *Heating and Process.* N.p., 22 Nov. 2016. Web. 07 Feb. 2017
[3] Lawrence, Chris. "Families Mark Seven Years since UBB Tragedy." WV MetroNews. West Virginia MetroNews Network, 05 Apr. 2017. Web. 06 Apr. 2017. <http://wvmetronews.com/2017/04/05/families-mark-seven-years-since-ubb-tragedy/>.
[4] Cardona, Libardo. "Colombian Coal Mine Blast Kills 16, Traps Dozens."Sandiegouniontribune.com. N.p., 17 June 2010. Web. 06 Apr. 2017. <http://www.sandiegouniontribune.com/sdut-colombian-coal-mine-blast-kills-16-traps-dozens-2010jun17-story.html>.
[5] Cardona, Libardo. "Colombian Coal Mine Blast Kills 16, Traps Dozens."Sandiegouniontribune.com. N.p., 17 June 2010. Web. 06 Apr. 2017. <http://www.sandiegouniontribune.com/sdut-colombian-coal-mine-blast-kills-16-traps-dozens-2010jun17-story.html>.
[6] Hannon, Ami, et al. "A sensor array for the detection and discrimination of methane and other environmental pollutant gases." *Sensors* 16.8 (2016): 1163.
[7] Ahuja, Dhiraj, and Deepa Parande. "Optical sensors and their applications." *Journal of Scientific Research and Reviews* 1.5 (2012): 060-068.
[8] Allsop, Thomas, et al. "Photonic gas sensors exploiting directly the optical properties of hybrid carbon nanotube localized surface plasmon structures."*Light: Science and Applications* 5 (2016): e16036.
[9] Meyyappan, M. "Carbon Nanotube-Based Chemical Sensors." *Small* 12.16 (2016): 2118-2129.
[10] Campbell, Mark L. "Kinetics of the termolecular reaction of gas phase Pd (a 1 S 0) atoms with methane." *Chemical physics letters* 365.3 (2002): 361-365.
[11] Campbell, Mark L. "Kinetics of the termolecular reaction of gas phase Pd (a 1 S 0) atoms with methane." *Chemical physics letters* 365.3 (2002): 361-365.
[12] Tan, Zhenquan, et al. "Arrangement of palladium nanoparticles templated by supramolecular self-assembly of SDS wrapped on single-walled carbon nanotubes." *Chemical Communications* 46.24 (2010): 4363-4365.
[13] Tan, Zhenquan, et al. "Arrangement of palladium nanoparticles templated by supramolecular self-assembly of SDS wrapped on single-walled carbon nanotubes." *Chemical Communications* 46.24 (2010): 4363-4365.
[14] Lu, Yijiang, et al. "Room temperature methane detection using palladium loaded single-walled carbon nanotube sensors." *Chemical Physics Letters*391.4 (2004): 344-348.
[15] Lu, Yijiang, et al. "Room temperature methane detection using palladium loaded single-walled carbon nanotube sensors." *Chemical Physics Letters*391.4 (2004): 344-348.
[16] Tan, Zhenquan, et al. "Arrangement of palladium nanoparticles templated by supramolecular self-assembly of SDS wrapped on single-walled carbon nanotubes." *Chemical Communications* 46.24 (2010): 4363-4365.
[17] Lu, Yijiang, et al. "Room temperature methane detection using palladium loaded single-walled carbon nanotube sensors." *Chemical Physics Letters*391.4 (2004): 344-348.
[18] "Methane Detectors Challenge." *EDF + Business.* Environmental Defense Fund, n.d. Web. 22 Apr. 2017. <http://business.edf.org/projects/featured/natural-gas/methane-detectors-challenge/>.
[19] *METHANE DETECTORS CHALLENGE.* Rep. Environmental Defense Fund, n.d. Web. 22 Apr. 2017. <http://www.edf.org/sites/default/files/mdc_rfp_final.pdf>.
[20] Wang, Yun, and John TW Yeow. "A review of carbon nanotubes-based gas sensors." *Journal of Sensors* 2009 (2009).
[21] Tvrdy, Kevin, et al. "A kinetic model for the deterministic prediction of gel-based single-chirality single-walled carbon nanotube separation." *ACS nano* 7.2 (2013): 1779-1789.

[22] Strano, Michael S., et al. "Nanobionic engineering of organelles and photosynthetic organisms." U.S. Patent Application No. 14/454,196.
[23] Qiguan Wang and Hiroshi Moriyama (2011). Carbon Nanotube-Based Thin Films: Synthesis and Properties, Carbon Nanotubes - Synthesis, Characterization, Applications, Dr. Siva Yellampalli (Ed.), InTech, DOI: 10.5772/22021. Available from: https://www.intechopen.com/books/carbon-nanotubes-synthesis-characterization-applications/carbon-nanotube-based-thin-films-synthesis-and-properties
[24] Duggal, Rajat, Fazle Hussain, and Matteo Pasquali. "Self-Assembly of Single-Walled Carbon Nanotubes into a Sheet by Drop Drying." *Advanced Materials* 18.1 (2006): 29-34.
[25] Wang, Yun, and John TW Yeow. "A review of carbon nanotubes-based gas sensors." *Journal of Sensors* 2009 (2009).
[26] Ueda, T., et al. "Development of carbon nanotube-based gas sensors for NOx gas detection working at low temperature." *Physica E: Low-dimensional Systems and Nanostructures* 40.7 (2008): 2272-2277.
[27] Tan, Zhenquan, et al. "Arrangement of palladium nanoparticles templated by supramolecular self-assembly of SDS wrapped on single-walled carbon nanotubes." *Chemical Communications* 46.24 (2010): 4363-4365.
[28] Di Crescenzo, Antonello, Valeria Ettorre, and Antonella Fontana. "Non-covalent and reversible functionalization of carbon nanotubes." *Beilstein journal of nanotechnology* 5.1 (2014): 1675-1690.
[29] *METHANE DETECTORS CHALLENGE.* Rep. Environmental Defense Fund, n.d. Web. 22 Apr. 2017. <http://www.edf.org/sites/default/files/mdc_rfp_final.pdf>.
[30] Trimboli, Joseph, and Prabir K. Dutta. "Oxidation chemistry and electrical activity of Pt on titania: development of a novel zeolite-filter hydrocarbon sensor." *Sensors and Actuators B: Chemical* 102.1 (2004): 132-141.

VI. APPENDIX

A. Experimental Set-Up

A.1 Methane gas sensing in aqueous phase

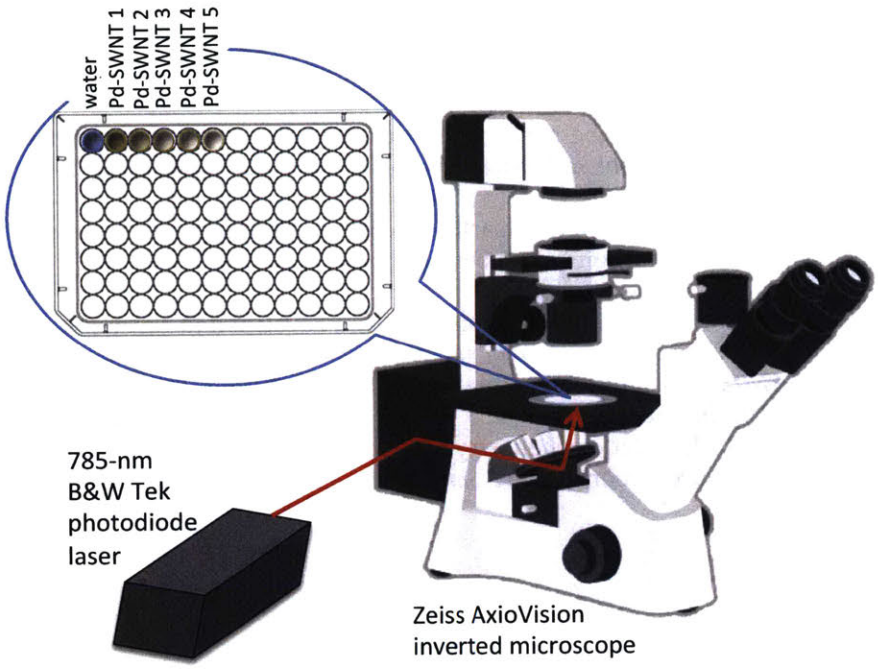

A.2 Methane gas sensing in solid phase (film)

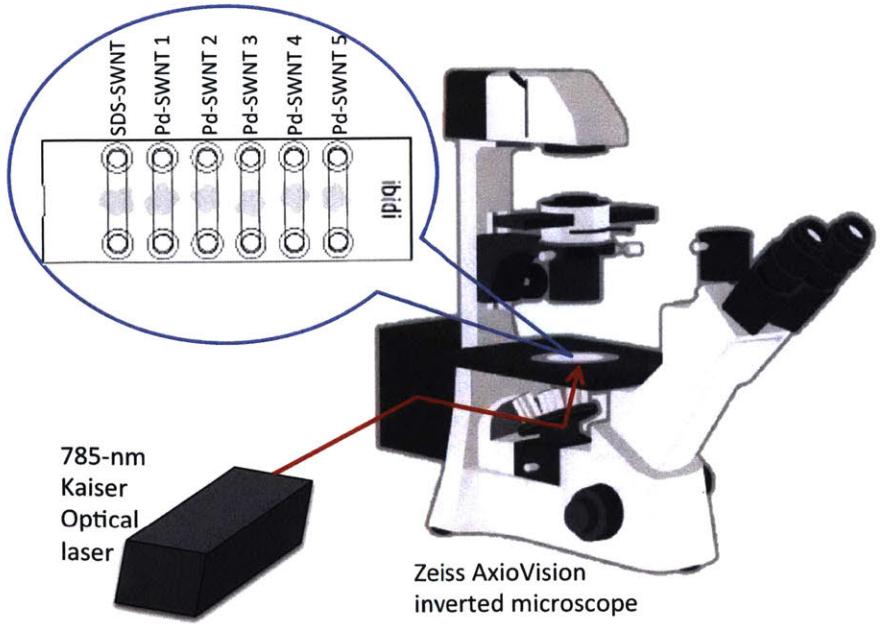

B. Data Processing

B.1 Calculation of Average Percent Recovery

Example: Solution Set A Pd-SWNT LOW

1. Maximum value determined per peak

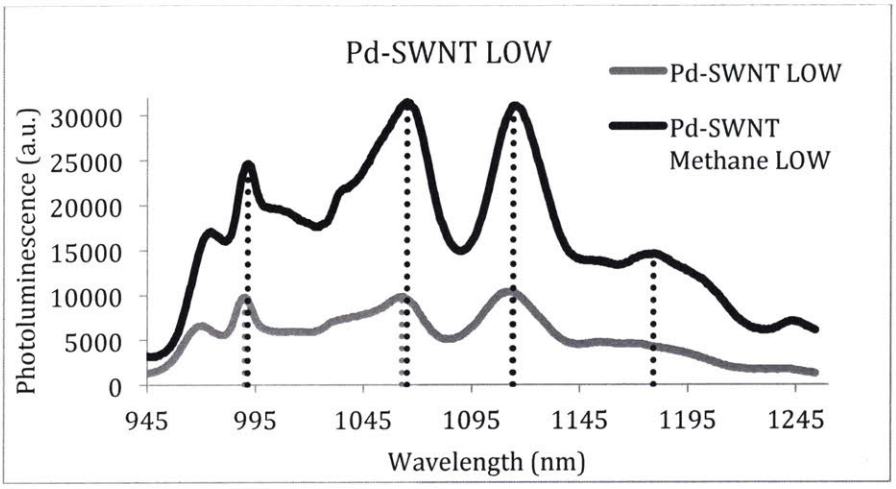

2. Percent recovery determined per peak according to the calculation below:

$$Percent\ Recovery = \frac{Methane\ Photoluminescence}{Pd \cdot SWNT\ Photoluminescence} \times 100\%$$

Example: Peak 1

$$Percent\ Recovery = \frac{24656}{9762} \times 100\% = 252.57\%$$

3. Average percent recovery determined by averaging each peak's recovery

	Pd-SWNT		Methane		
	Wavelength (nm)	Photo-luminescence (a.u.)	Wavelength (nm)	Photo-luminescence (a.u.)	Percent Recovery
Peak 1	990.197	9762	991.409	24656	252.57%
Peak 2	1062.841	9841	1065.259	31513	320.22%
Peak 3	1113.583	10367	1114.187	31100	299.99%
Peak 4	1179.294	4261	1179.294	14593	342.48%
					303.82%

B.2 Calculation of fluorescence of solid phase (films)

Example: Solution Set B Pd-SWNT

1. Open WinSpec file of all frames in ImageJ
2. Create an ellipsoid selection of heigh 150 pixels and width 320 pixels at center location (160, -75)

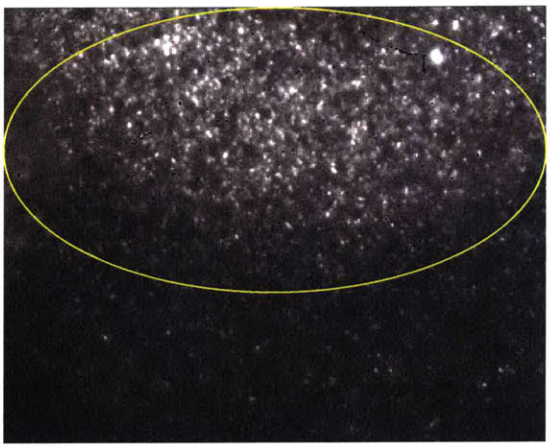

3. Plot "Z Axis Profile" from ellipsoid selection, giving as output the average fluorescence (Col.2) in the ellipsoid for each time frame (Col.1)
4. The fluorescence data (Col.2) is shifted by a value such that the minimum value in the column is zero (Column 3)
5. A rolling average window is then calculated (Column 4) with N=10.
6. This data is then scaled by the maximum height of all of the data in the set so that the resulting values are all normalized on the same scale (Column 5).

Col. 1	Col. 2	Column 3	Column 4	Column 5
Frame	Pd-SWNT 3 Methane Fluorescence	Shifted to minimum	Rolling Average Window, N=10	Scaled by maximum height
Raw Data	Raw Data	Col 2 - MIN(Col 2)	AVERAGE(R1-R10)	Column 4/500
1	4117.8032	111.791	69.90727	0.13981454
2	4049.0417	43.0295	61.77556	0.12355112

3	4021.9639	15.9517	60.15259	0.12030518
4	4065.7158	59.7036	65.398	0.130796
5	4101.395	95.3828	63.65293	0.12730586
6	4107.2773	101.2651	61.60357	0.12320714
7	4062.1426	56.1304	56.63641	0.11327282
8	4083.7112	77.699	56.79813	0.11359626
...	...	...	...	...

C. Data

C.1 Solution Set B Aqueous Phase response to methane gas

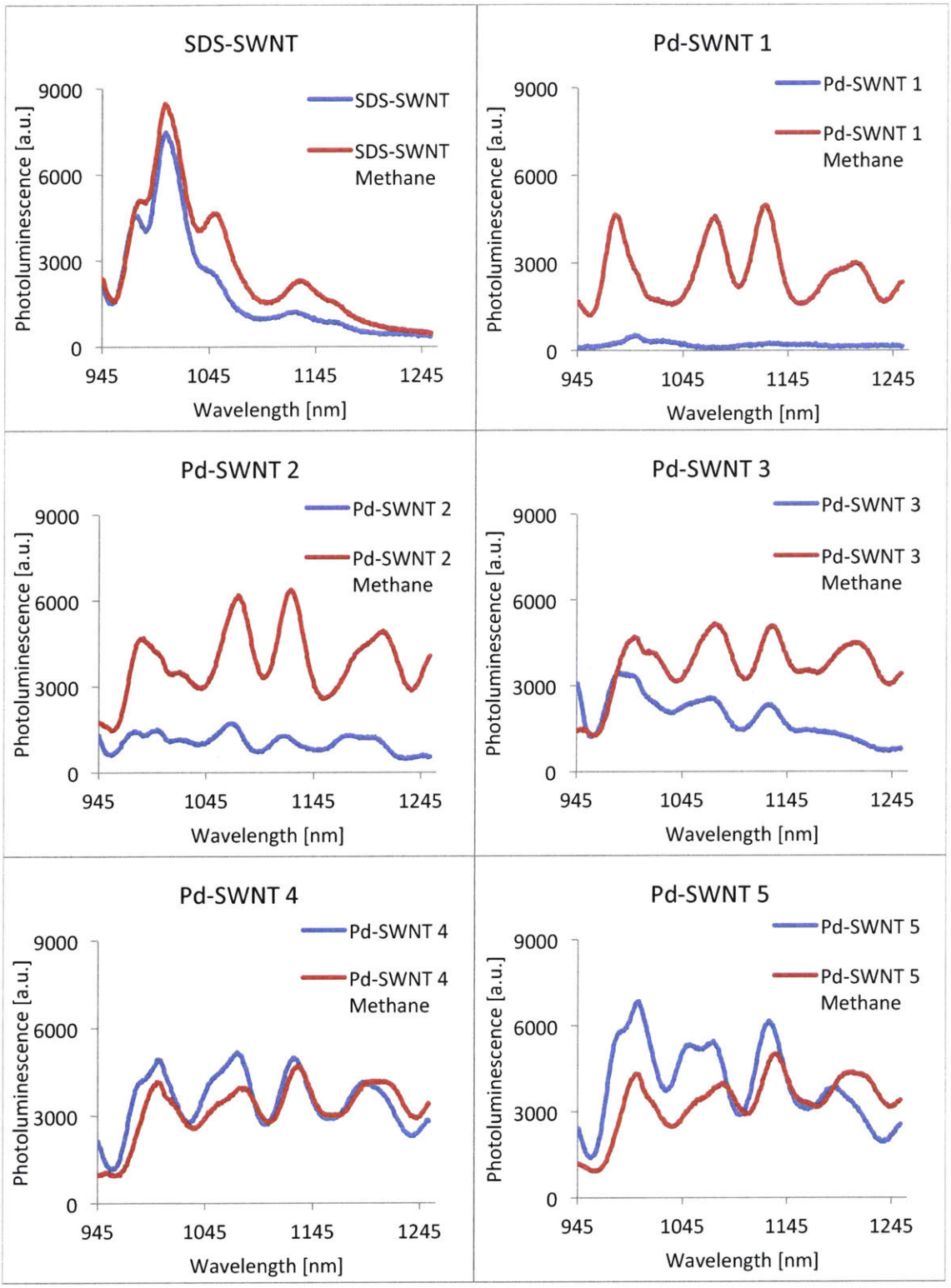

C.2 Solution Set B film fluorescence upon photoexcitation

Fluorescence of (a) SDS-SWNT; (b) Pd-SWNT 1; (c) Pd-SWNT 2; (d) Pd-SWNT 3; (e) Pd-SWNT 4; (f) Pd-SWNT 5 under continuous photoexcitation by a785nm, 200mW near infrared laser.